JACS
JOURNAL OF THE AMERICAN CHEMICAL SOCIETY

Article

pubs.acs.org/JACS

Temporal Variation of a Protein Folding Energy Landscape in the Cell

Anna Jean Wirth,[†] Max Platkov,[†] and Martin Gruebele*[,†,‡]

[†]Department of Chemistry and [‡]Department of Physics and Center for Biophysics and Computational Biology, University of Illinois, Urbana, Illinois 61801, United States

Supporting Information

ABSTRACT: Chemical reaction rate coefficients and free energies are usually time-independent quantities. Protein folding *in vitro* is one such reaction with a fixed energy landscape. However, in the milieu of the cell, the energy landscape can be modulated in space and time by fluctuations in the intracellular environment such as cytoskeletal rearrangements, changes in biomolecule concentrations, and large scale cellular reorganization. We studied the time dependence of the folding landscape of a FRET-labeled enzyme, yeast phosphoglycerate kinase (PGK-FRET). Living U2OS cells served as our test tube, and the mammalian cell cycle, a process strictly regulated in time, served as our clock. We found that both the rate of folding and the thermodynamic stability of PGK-FRET are cell cycle-dependent. We also assayed folding rates of PGK-FRET in spatial proximity to and far away from mitotic chromosomes. Our results show that expedited folding in DNA-rich regions cannot account for the faster rate of PGK-FRET folding in mitotic cells.

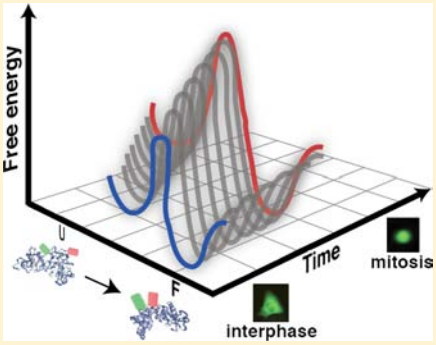

INTRODUCTION

Like all chemical reactions, protein folding is dependent on its environment. Solvation, pH, crowding, and ionic strength are just a few of the well-documented factors that affect the stability and folding rates of proteins in the test tube.[1−3] Nonetheless, the energy landscape traversed by proteins during folding is usually considered to be constant in time, unless subject to artificial modulation.[4] Yet inside the cell, where proteins are manufactured and may live out their entire functional life cycle before being degraded, the environment is constantly changing over time. The prime example is the cell cycle itself,[5] when the cell undergoes drastic changes in internal morphology between periods of quiescence and cell division. Here, we use protein stability and folding kinetics to probe this time-dependent cytoplasmic environment. The cell cycle could purposely modulate protein folding and function in ways that are adaptive, the functional abundance of tumor-suppressor p53 being a prime example.[6]

Here we use the folding reaction of the ubiquitous ATP-producing enzyme phosphoglycerate kinase (PGK) to probe the cell cycle of U2OS bone cancer cells in interphase (G1/S) and mitosis (pro/metaphase). As illustrated in Figure 1, PGK is a 415 residue enzyme with two domains in the crystal structure,[7] although measurements in cells and in Ficoll crowder indicate that it is even more compact when folded in the crowded milieu of the cell.[8] We label the enzyme with two fluorophores at the N and C termini, so the thermal stability and folding rate of the resulting PGK-FRET construct can be detected inside live cells by change in Förster Resonance Energy Transfer (FRET) upon thermal unfolding.[9] We then combine cell cycle arrest with transient transfection as a potentially higher throughput method than cell line generation to look at time-dependent protein stability and folding kinetics. By measuring changes of the protein melting temperature and folding rate at different times during the cell cycle, we can quantify the temporal variation of the PGK-FRET energy landscape as the cytoplasmic environment changes.

We find that mitotic cells increase the stability of PGK-FRET by about 5 kJ/mol relative to interphase cells. We also conclude that the lower viscosity of mitotic cells overcomes a small increase of the activation barrier during mitosis, leading to faster folding kinetics in mitotic cells relative to interphase cells.

The same trends were observed previously when PGK-FRET was localized to the nucleus by a nuclear localization tag.[10] It was hypothesized that DNA−protein interaction rather than simple crowding (excluded volume) differences might underlie the greater stability of PGK the nucleus. Our data is consistent with this earlier proposal, but we show that this scenario cannot by itself explain the mitotic-interphase folding rate difference: imaging of PGK-FRET relaxation kinetics in DNA-rich and DNA-poor regions of the cell reveals at best a small variation of rate coefficient.

MATERIALS AND METHODS

Cell Cycle Arrest. Osteosarcoma (U2OS) cells were grown by standard practices. Cells were arrested at the G1 and S border of interphase with a double thymidine block:[11] 12 h incubation in 2 mM thymidine (Sigma) supplemented DMEM with 1% PS and 10% FBS, was followed by 12 h in thymidine free media, and 12 h of incubation again with thymidine. Cells were arrested in mitosis, between prometaphase and metaphase, by addition of nocodazole[11] (Sigma): 12 h in DMEM with 1% PS, 10% FBS, and 100 ng/mL nocodazole. The degree of cell cycle arrest was assayed with flow cytometry (Figure S1).

Received: August 22, 2013
Published: December 4, 2013

dx.doi.org/10.1021/ja4087165 | J. Am. Chem. Soc. 2013, 135, 19215−19221

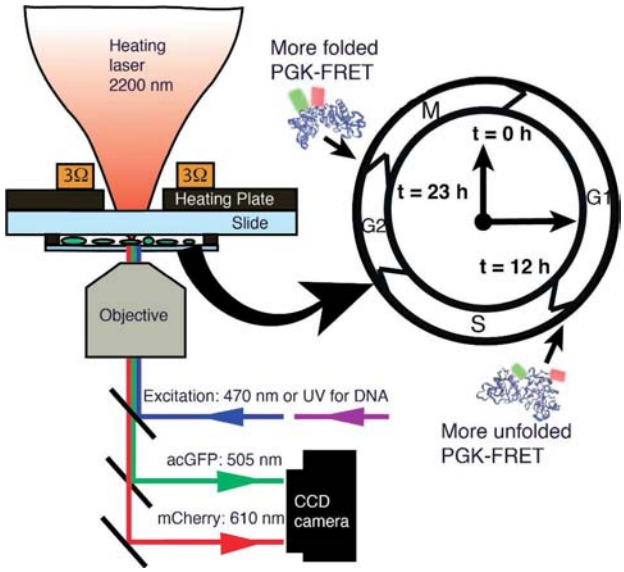

Figure 1. Schematic of the Fast Relaxation Imaging (FReI) experiment coupled to the cell cycle as a clock. U2OS cells divide every 24 h. At the beginning of gap 1 (G1) or $t = 0$, cells grow. In synthesis (S) or $t =$ 12 h, the genome of the cell is duplicated. In gap 2 (G2), the cells continue to grow. In mitosis (M) or $t = 23$ h, the cell condenses its chromosomes, and finally divides into two daughter cells. Cells arrested at the end of G1 and at the beginning of M are temporally separated by about 11 h. Such cells, transfected with PGK-FRET as a probe protein, are imaged to look at changes in stability and folding kinetics during the cell cycle (schematic proteins with arrows pointing at G1 and M). To probe protein stability and kinetics, a green fluorescent donor label is excited by a 470 nm LED, and green donor as well as red acceptor emission are imaged into channels with millisecond time resolution: acGFP (donor) at 505 nm and mCherry (acceptor) at 610 nm. The resulting movies of protein thermodynamics or kinetics are collected during different parts of the cell cycle. IR heating for temperature jump kinetics and thermal unfolding titrations is provided by a 2200 nm laser.

Transfection and Plasmid Constructs. The plasmid constructed for transfection encoded a FRET-labeled, destabilized, enzymatically active yeast phosphoglycerate kinase (PGK) mutant described previously.[9] A destabilized probe protein allows us to assay the folding within a temperature range acceptable for cell survival, and well below the melting temperature of the FRET labels. The fusion protein consisted of an N-terminal 6 histidine tag, AcGFP1, the destabilized Y122W W308F W333F PGK mutant, and mCherry at the C terminus. The fusion protein was cloned into the pDream 2.1 vector (Genscript) which contains both a T7 and CMV promoter for dual expression in bacterial and mammalian cells. For temperature calibrations, an mCherry-alone construct, also in pDream, was used and consisted of an N-terminal 6-histidine tag and mCherry.

Cells were transfected with 0.6 μg of plasmid per coverslip via Lipofectamine (Invitrogen) according to the manufacturer's protocol. For interphase arrest, cells were transfected during the 12 h thymidine-free incubation period. Cells were imaged immediately following the second 12 h thymidine incubation period. For mitotic arrest, cells were transfected 6 h before addition of nocodazole and imaged immediately after 12 h of incubation with the arresting agent. In both cases, the arresting agent was not present during imaging to maintain cell viability during experiments.

Fast Relaxation Imaging. Fast relaxation imaging has been described in detail elsewhere, and is illustrated in Figure 1.[9] Briefly, the model protein PGK-FRET consists of PGK sandwiched between a FRET pair: green fluorescent AcGFP1 as a donor at the N-terminus, and red fluorescent mCherry as an acceptor at the C-terminus, both with melting points >70 °C. PGK-FRET has been studied extensively *in vitro* and in cells, making it a suitable model system for cell-cycle-dependent protein folding.[9,10] It can change in size from about $r = 2$ nm C to N terminal distance in the folded state, to as much as $r = 17$ nm C to N distance upon unfolding to a random coil.[12] (The actual unfolded state inside cells will be more compact.) These values of r are a good match for the Förster distance R_0 (~5 nm) of the two chromophores.

The donor fluorescence intensity D increases, and the acceptor fluorescence intensity A decreases when the protein unfolds because the two fluorescent tags are further apart in the unfolded state. Thus the ratio D/A increases, the FRET efficiency $E = [1 + (D/A)]^{-1}$ decreases, and the difference $D - A$ increases upon unfolding.

PGK-FRET, as a consequence of its large fluorescent tags, shows slightly different folding stability and kinetics than the unlabeled PGK construct.[10] Therefore, all comparisons among different environments are made with the same FRET construct, never with wild type PGK.

U2OS cells expressing our probe protein were imaged on a modified epifluorescent microscope, a schematic of which is shown in Figure 1. After excitation at 470 nm, emission was split into red and green channels and imaged side by side on a CCD camera at 24 frames per second (fps) for thermodynamics and 60 fps for kinetics. For Hoechst labeling experiments, the dye was excited at 365 nm and resulting 465 nm emission collected in the green channel.

Thermal unfolding was used to gauge PGK-FRET stability in G1 and M. Thermal denaturation traces were collected through stepped laser heating by an IR laser mounted above the sample stage as described previously.[13] An entire thermodynamic trace is acquired within 5 min. In-cell temperatures were calibrated using the known temperature dependence of the mCherry quantum yield (Figure S2). Thermodynamic traces are plotted as the donor to acceptor ratio D/A vs temperature. D/A conveniently cancels out the temperature dependence of the donor quantum yield, it connects the FRET label separation r and the Förster radius R_0 by $r = (D/A)^{1/6} R_0$, and it does not require knowledge of $R_0(T)$ in cells, which is unknown. The SI discusses the temperature dependence of R_0 and derives r as a reaction coordinate, showing that our conclusions are robust, whether r or D/A is used.

Although PGK is a two domain multistate folder,[14,15] in thermal melts PGK-FRET behaves like an apparent two-state folder.[9] Thus, the thermodynamic traces were fitted to a simple two-state model assuming linear baselines for the folded and unfolded states to extract the most robust thermodynamic parameters, in particular, the effective melting temperature T_m of the protein (see SI). As shown in Figure 2 of ref 10, the baselines arise mostly because of the nearly linear temperature-dependent chromophore quantum yields, and when they are eliminated by correcting for temperature-dependent quantum yield, very similar thermodynamic parameters are obtained.

Repeated measurements of thermodynamics *in vitro* and in-cell by two different methods, slow heating of the stage and stepped laser heating,[10,13,16] show that relative changes of temperature can be calibrated with a standard deviation of 0.5 °C and a 2σ error of the mean of 0.6 °C, but absolute temperatures in-cell ranged from 38.8 to 42 °C with a much larger standard deviation of 1.5 °C. The stepped laser heating used here cannot be calibrated accurately for comparing *in vitro* measurements with in-cell measurements (see SI). For reference, the PGK-FRET *in vitro* melting temperature difference in Table 1 is the average of all available literature values,[10,13,16] and the uncertainty in the *in vitro* ΔT_m reported in Table 1 is based on the uncertainty of all literature measurements.

Kinetics at constant temperature after a jump were measured in G1 and M by applying a small (4 °C), 6 s duration temperature jump achieved by a shaped infrared laser heating pulse with about 20 ms resolution (Figure S5). The slide temperature was maintained 1 °C below the average PGK-FRET melting temperature in either the interphase or mitotic cells prior to T-jumps. Thus, kinetics in the two populations were carried out under equal average stability conditions in the two environments. The sample slide temperature was maintained within a thermostable cavity, and thermal stability was achieved by a PID (proportional-integral-derivative loop with 0.1 °C accuracy, see SI). Fine control of the starting temperature for kinetic

dx.doi.org/10.1021/ja4087165 | J. Am. Chem. Soc. 2013, 135, 19215−19221

Table 1. Effective Thermodynamic Parameters[a]

	ΔT_m (°C)	$\Delta H_{U\to F}$ (kJ mol^{-1})	$\Delta S_{U\to F}$ (kJ mol^{-1} K^{-1})
Mitotic	+2.5 ± 1.0	−485 ± 54	−1.54 ± 0.17
Interphase	0	−665 ± 37	−2.13 ± 0.12
In vitro	−2.5 ± 0.6	−459 ± 201	−1.48 ± 0.65

[a]All values based on two-state fits. Uncertainty reported is two standard deviations of the mean (2σ). *In vitro* values are from refs 10, 13, and 16.

experiments allowed for relatively high throughput, constant free energy measurements between the two cell populations.

Folding kinetics are expressed as a donor to acceptor difference, $S(t) = D(t) - aA(t)$, where $D(t)$ and $A(t)$ are the time dependent donor and acceptor intensities and a is the initial donor to acceptor ratio, and were fitted to a stretched exponential signal $s(t) = A \exp[-(kt)^{\beta}]$. As discussed in detail in ref 10, the donor to acceptor difference is a useful FRET measure for kinetics because the signal is directly proportional to the population of folded protein, and canceling temperature dependence is not an issue. Unlike the thermodynamics of PGK-FRET, the folding kinetics show some measurable deviations from two-state behavior which can be represented by $\beta < 1$ in the simplest case (or by a multiexponential fit with more adjustable parameters).[17]

Regional Folding Kinetics. In regional kinetic experiments with subcellular resolution, mitotic chromosomes were stained with Hoechst 33258, a UV excitable intercalating dye. Mitotic arrested cells on coverslips were incubated with 3 μg/mL Hoechst 33258 (Invitrogen) in OptiMEM minimal media (Gibco) supplemented with 10% FBS and 100 ng/mL nocodazole for 30 min at 37 °C and 5% CO_2. Cells were rinsed gently two times with PBS (Lonza) before imaging. Staining was carried out during the last 30 min of nocodazole incubation.

To identify regions of mitotic cells that were rich in DNA, cells were imaged under UV excitation after Hoechst staining. Then, the folding kinetics experiment described in the previous subsection was carried out under 470 nm excitation. UV and blue images were aligned by cross-correlation (Figure S7). The overlay was used to identify DNA-rich and DNA-poor regions. Pixels corresponding to these two regions were averaged to yield spatially resolved kinetic traces.

Mitotic cells are spherical (Figure 2b); therefore, some of the signal in the identified DNA-rich region comes from areas that are not DNA-rich above and below the chromosomes. To compensate for this loss in experimental sensitivity, the depth of the chromosomes relative to the depth of the cell was used to calculate the proportion of observed signal in the DNA-rich region that comes from DNA-rich and DNA-poor parts of the cytoplasm. A simulation was then used to correct the observed DNA-rich folding rate so that signal from DNA-poor regions is excluded (see SI for further details).

RESULTS

Harnessing the Cell Cycle "Clock" To Measure the Time-Dependence of the Intracellular Protein Folding Landscape. Immortalized cell lines, such as the U2OS line used here, constantly move through the cell cycle in a strictly time-regulated fashion completing a full cycle every 24 h. Figure 1 illustrates the time dependence of this process as studied here. Arresting cells at a stage of the cell cycle allows for characterization of the intracellular environment across an entire population of cells at a single point in time.

We used this concept to develop a technique to study the time dependence of an intracellular protein folding landscape. Using common molecular biology techniques,[11] we arrested cells just before DNA synthesis begins, in interphase, which corresponds to $t \sim 12$ h relative to the beginning of the cell cycle. To access a later time point, $t \sim 23$ h, we arrested cells in the early stages of mitosis. Degree of arrest attained for both time points was verified by flow cytometry (Figure S1). We combined this cell-cycle arrest approach with transient transfection to enable relatively rapid study of different proteins without the need to generate unique cell lines expressing a labeled protein of interest.

Thermodynamic Stability of PGK-FRET is Time-Dependent. The thermodynamics of PGK-FRET unfolding was measured in the cytoplasm of 18 mitotic cells and 9 interphase cells (Figure 2 and SI). Fits of the two data sets yielded a T_m of 41.3 ± 0.8 °C for mitotic cells and 38.8 ± 0.6 °C for interphase cells. PGK-FRET is more stable in mitotic cells, as evidenced by their 2.5 ± 0.6 °C higher mean effective melting temperature T_m compared to interphase cells (Table 1).

The square root of the variance of T_m, which describes the degree of cell-to-cell variation rather than relative measurement uncertainty, was 1.5 °C in mitotic cells and 0.9 °C in interphase

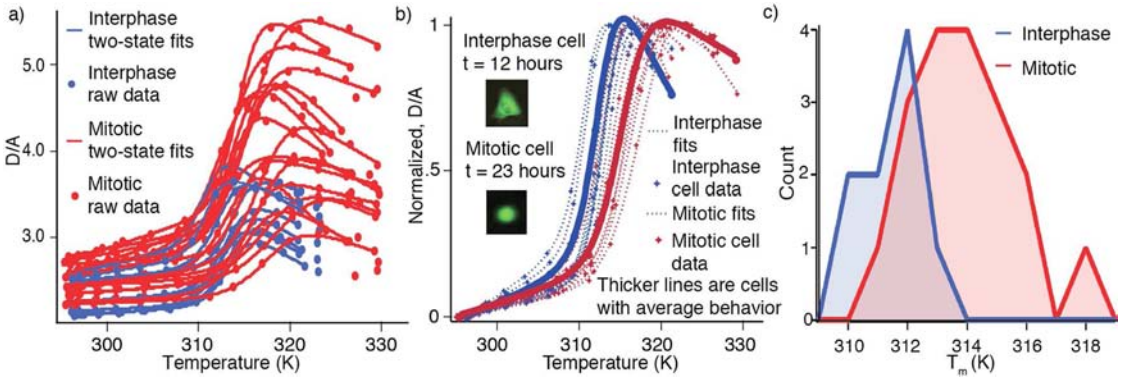

Figure 2. PGK-FRET thermal melts as a function of the cell cycle in mitotic- and interphase-arrested U2OS cells. Larger donor/acceptor (D/A) ratios correspond to unfolded protein. (A) Raw thermodynamic data. Un-normalized, baseline unadjusted mitotic (18 cells), and interphase (9 cells) data is plotted with corresponding two-state fits. (B) For clarity, 9 randomly selected mitotic cells and all 9 interphase cells are displayed and the data is scaled from 0 to 1. The highlighted traces are for two cells that exemplify the average behavior of each cell cycle population. Insets show morphology of an interphase and a mitotic cell. Data is not corrected for temperature dependence of the Förster constant (see SI for corrected data, and a plot in terms of end-to-end distance r instead of D/A). (C) Histogrammed fitted T_m values for all interphase and mitotic cells showing overlapping populations and greater heterogeneity in mitotic cells. Note that some of this heterogeneity could come from variations in the timing of the cell cycle arrest.

dx.doi.org/10.1021/ja4087165 | J. Am. Chem. Soc. 2013, 135, 19215−19221

cells, indicating greater cell to cell variation in mitotic cells (see SI for statistical significance test). The greater heterogeneity of mitotic cells (Figure 2c) may arise from cell-to-cell differences in cellular structure only present during mitosis. Mitosis is a far more morphologically diverse phase than the G1/S border, with varying degrees of chromatin compaction or extent of mitotic spindle formation. Heterogeneity differences may also rise from the faster time-scale of mitosis. The many morphologically diverse events of mitosis occur over the course of an hour, so slight differences in cell-cycle timing could produce greater heterogeneity. Interphase cells, on the other hand, experience no dramatic morphological changes for many hours, so the exact timing of cell-cycle arrest has less of an effect.

Thermodynamic fits also extracted the effective two-state difference in enthalpy and entropy of PGK-FRET unfolding between interphase and mitotic cells (see SI). Both the Van't Hoff enthalpy ($\Delta H_{U\rightarrow F}$) and entropy ($\Delta S_{U\rightarrow F}$) of folding are greater for PGK-FRET in interphase cells than in mitotic cells (Table 1).

Compactness of the Unfolded State of PGK-FRET is Time-Dependent. Protein compactness over the course of a thermodynamics experiment can be assessed by the D/A ratio since $r = (D/A)^{1/6} R_0$. Below the unfolding temperature, interphase and mitotic cells show a similar value of D/A 2.33 ± 0.13 for interphase cells and 2.51 ± 0.17 for mitotic cells (Figure 2A). However, upon unfolding the maximum D/A of PGK-FRET ranges from 3.1 to 5.5 in mitotic cells, but only from 2.9 to 3.6 for interphase cells. This implies that the unfolded state of PGK-FRET is more expanded in mitotic cells than in interphase cells, or at least that the FRET labels are less crowded.

PGK-FRET Folding Kinetics Varies with Cell Cycle. Folding/unfolding relaxation kinetics traces of PGK-FRET were collected on 3 mitotic cells and 3 interphase cells via 4 °C temperature jumps from 1 °C below their respective T_m (Figure 3, Figure S5). The resulting kinetic traces of PGK-FRET relaxation were fit to stretched exponentials Signal ~ $\exp[-(kt)^{\beta}]$ as described in Methods and SI. The observed relaxation rate k equals about twice the folding rate for jumps close to the melting temperature. The stretching factor β describes the deviation from two-state behavior, or multiple populations with different relaxation rates. Mitotic cells showed faster relaxation and a greater deviation from two-state folding with a mean k of 0.62 ± 0.04 s^{-1} and β of 0.84 ± 0.01 compared to interphase cells with k of 0.44 ± 0.01 s^{-1} and a β of 0.95 ± 0.03.

To investigate whether the 'kinetic stretching' in mitotic cells is just due to averaging over different rates in different parts of the cell, or reflects a change in folding mechanism throughout the cell, we examined folding kinetics separately in two different regions of mitotic cells: a DNA-rich area whose location was identified by staining with Hoechst 33258 labeling, and the remaining DNA-poor region (Figure 4 and SI Figures S7 and S8). A difference between DNA-rich and -poor regions is also of interest because faster folding of PGK-FRET has been observed in the nucleus of interphase cells than in the cytoplasm,[10] so protein–DNA interaction in mitotic cells, where the nuclear envelope has dissolved, could be the reason for the different rates observed in Figure 3. The difference between the DNA-rich kinetics (orange in Figure 4) and DNA-poor kinetics (green in Figure 4) is far too small to account for the faster mitotic kinetics in Figure 3. When we take into account that the DNA does not occupy the whole column probed by our diffraction-limited imaging, the extrapolated DNA-only rate (black dotted curve in Figure 4) is 22% faster on average in mitotic cells, with a ±24% root-mean-square variation among 5 cells measured (see SI Table S4 and Figure S8). Thus, our results are consistent with the earlier proposal that DNA-PGK-FRET interaction could speed up folding relaxation kinetics,[10] but they cannot account for the mitotic-interphase difference observed here in Figure 3.

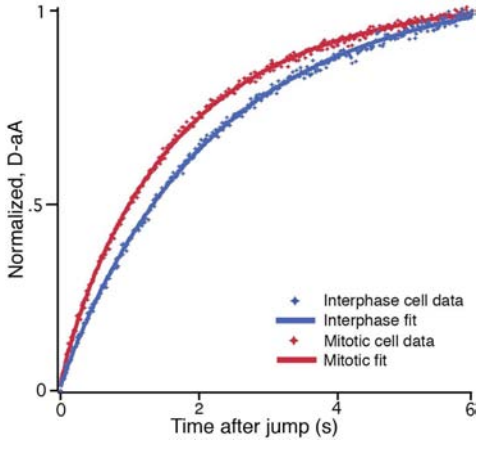

Figure 3. Averaged mitotic and interphase kinetic traces. As shown here, the fluorophore temperature response has been subtracted from the data and the data normalized. Figure S6 shows raw kinetic data traces for all cells, with the fluorophore temperature response included. The T-jump relaxation was fit to yield PGK-FRET relaxation rates k and an exponent β that describes deviations from two-state kinetics (see SI). T-jump begins at t = 0 s, and higher $D - aA$ means more unfolded protein. Mitotic cells (red) show a faster relaxation rate than interphase cells (blue).

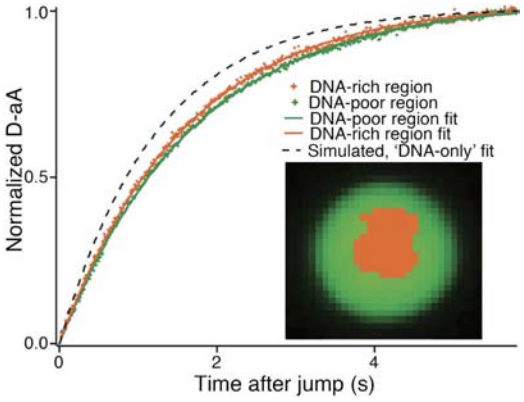

Figure 4. Spatially resolved kinetics of PGK-FRET unfolding in mitotic cells. Inset: DNA-rich and -poor regions were identified by Hoechst staining of the DNA: UV-excited images showing chromosomes (orange) were merged with the FRET-detected kinetic images (green) of mitotic cells to determine regional boundaries. Kinetic traces: PGK-FRET unfolding kinetics with fits in DNA-rich and DNA-poor regions. The simulated, DNA-rich region fit corresponds to the DNA-rich signal with contributions from DNA-poor regions removed (see Methods and SI). The DNA-rich and DNA-poor data above is the S:N weighted average of the DNA-rich or DNA-poor regions for 5 cells.

dx.doi.org/10.1021/ja4087165 | J. Am. Chem. Soc. 2013, 135, 19215–19221

Diffusion Coefficient for Folding Increases during Mitosis. Like any chemical reaction in a solvent environment, protein folding rates depend on the prefactor and the activation barrier. The temperature dependence of the folding rate can be described by the Arrhenius equation:

$$k(T \approx T_m) = 2k_m \exp(-\Delta G^{\dagger}/RT) \quad (1)$$

where $\Delta G^{\dagger}$ is the free energy barrier for folding and k_m is the prefactor, which depends on internal friction of the polypeptide chain and on the material properties of the solvent, i.e., viscosity.[18,19] The factor of 2 in eq 1 accounts for the fact that near the T_m, where our experiments are carried out, the observed relaxation rate coefficient is the sum of equal folding and unfolding rate coefficients, or $k = k_f + k_u \approx 2k_f$.

A time-dependent energy landscape (barrier) and prefactor (diffusion) can contribute the observed time-dependent rate of reaction as the cell cycle progresses, and their relative contributions can provide insight into the mechanism underlying the rate differences between the two populations studied here.

Using Phi-value analysis,[20] we calculated the relative contributions of landscape vs diffusion to the observed folding rates in interphase and mitotic cells. Phi values describe how much the activation free energy of a reaction changes when the free energy of the reactant (here: folded protein) changes because of a mutation or, in our case, a change in the cellular environment. For example, $\Phi = 1$ implies that stabilization of the native state in mitotic cells lowers the activation energy by an equal amount, whereas $\Phi = 0$ implies that stabilization of the native state has no effect. The average Phi value for a single point mutation in a protein is 0.3,[21,22] and we assume that the effects of a changing cellular environment can be approximated by this same Phi value.[9]

To assign an upper and lower limit to calculated changes of the activation barrier and diffusion coefficient between interphase and mitotic cells, two extreme Phi value scenarios were considered. In the first, we assumed that most energy landscape differences between mitotic and interphase cells arise from free energy differences in the folded state (Phi = 0.7), and in the second, we assumed the complement: most changes result from free energy variations of the unfolded state (Phi = 0.3). Given the structural similarity of the folded states and the structural difference in the unfolded states in Figure 2B, the latter scenario is more likely.

In both scenarios, the activation barrier for folding is higher in mitotic cells than in interphase cells (see SI for details of the calculations). In other words, if the activation barrier alone were to control folding rates, PGK-FRET would fold faster in interphase cells than mitotic cells. Yet, the opposite is observed in Figure 3. This indicates that the prefactor more than makes up for the slightly higher barrier in mitotic cells or, in other words, the difference in prefactors indicates that diffusion for the folding reaction is 1.5−1.7 times faster in mitotic cells than in interphase cells.

DISCUSSION

The lives of cells are dynamic by nature—biomolecule and ion concentrations fluctuate and cellular structure is reorganized across many cellular processes—and one must consider whether such changes influence the biophysical and chemical properties of the intracellular environment enough to affect the energetics of protein function or folding with respect to time. Ideally, one would study such effects *in vitro* where experiments have improved signal and allow for greater manipulation of variables. Unfortunately, the cellular milieu is simply too complex to reconstruct in the test tube, at least at this point in time, particularly when one is interested in dynamics.

The folding free energy landscape of proteins *in vivo* is influenced by the intracellular environment.[10,23] To measure the time dependence of a folding landscape, we used living cells as our test tube and a biological process, the cell cycle, as our clock. We studied a model protein, FRET-labeled yeast phosphoglycerate kinase, because its folding both *in vitro* and in the cell is well understood. We found that PGK-FRET is stabilized at a later time in the life of a cell, mitosis, compared to an earlier time, interphase. This is the first direct evidence that a protein energy landscape can fluctuate over time inside cells. We also found that our probe protein folds more rapidly during mitosis due to an increased prefactor (faster diffusion) overcoming an increased barrier (energy landscape). Finally, we found that the rate effects are not associated with protein−DNA proximity as previously postulated for PGK localized to the nucleus,[10] so the exact mechanism behind these changes in stability and folding kinetics remains to be unraveled.

The time-dependent changes in the folding landscape can be rationalized by three factors: (1) cell cycle-dependent excluded volume, an entropic effect; (2) variation in the interaction between PGK-FRET and the intracellular environment, which can make both enthalpic and entropic contributions; and (3) changes in the degree of spatial heterogeneity in folding environments.

To apply these three factors to our data, we will make the assumption that the folded states of PGK-FRET are similar in mitotic and interphase cells (model in Figure 5). This assumption is justified by the similar range of D/A values in these two environments (Figure 2A). In contrast, the denatured state has a larger average D/A value in mitotic cells than in interphase cells, consistent with a less compact denatured state in mitosis than during interphase.

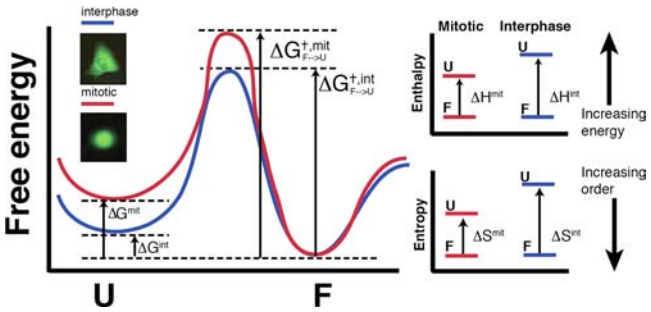

Figure 5. Schematic of proposed time-dependent energy landscape changes. Left panel: Free energy of PGK-FRET's folded state is similar between interphase and mitotic cells. The difference in thermodynamic stability arises from the greater instability of the unfolded state in mitotic cells, which pushes the equilibrium toward the folded state. The activation barrier for folding is higher in mitotic cells. Right panels: Mitotic cells show enthalpic stabilization of the unfolded state, which destabilizes the folded state. However, the unfolded state of mitotic cells is more ordered than in interphase cells, a stabilizing effect for the folded state that overcomes the destabilizing enthalpic effects.

(1). The cellular environment is more crowded than *in vitro*. But how do two in-cell environments separated by time differ from one another?

dx.doi.org/10.1021/ja4087165 | J. Am. Chem. Soc. 2013, 135, 19215−19221

Three lines of evidence indicate that excluded volume (macromolecular crowding) decreases as the cell cycle progresses from interphase to mitosis. First of all, the denatured state becomes less compact as the cell progresses from interphase to mitosis, as expected for less crowding. Second, the enthalpy and entropy of folding during mitosis more closely resemble the *in vitro* data measured in buffer (Table 1). Most compelling is the kinetic data. Our Phi value analysis indicates that mitotic cells have slightly higher activation barriers for folding and ∼1.6 times faster intramolecular diffusion than interphase cells, both expected for reduced crowding.[24,25] Thus, we conclude that mitotic cells are less crowded than interphase cells. The altered cytoskeletal structure, evident in the round shape of mitotic cells in Figures 2, 4, and 5, could be a reason for decreased crowding in mitotic cells.

(2). Usually increased melting temperatures of proteins are explained by increased crowding. If crowding decreases during mitotis but T_m increases (Table 1), another factor must be responsible. We believe that increased interaction of the unfolded state with the intracellular environment is a good candidate. First of all, the denatured state is less compact during mitosis, giving the unfolded polypeptide chain more opportunity to interact with its environment. In Table 1, the effective enthalpy of the denatured state is significantly lower during mitosis than interphase, consistent with increased binding of the denatured state to macromolecular surfaces, solvated ions, or other microstructure in the cell. (The same is incidentally true *in vitro*, indicating some interaction between FRET labels and PGK.)

A lower enthalpy of the denatured state alone would tend to decrease T_m during mitosis, so it must be offset by entropy. Indeed, in Table 1 the effective entropy of the unfolded state is significantly lower during mitosis. This is also consistent with increased interactions of the unfolded polypeptide chain, 'sticking' to other macromolecules in its environment, including the GFP and mCherry labels attached to the PGK. In this scenario, crowding is reduced in the mitotic state, and the resulting more extended unfolded state of PGK sticks to other cellular components, decreasing its enthalpy, but even more its entropy, thus destabilizing the unfolded state and increasing T_m.

Favorable enthalpic interactions between a protein's unfolded state and biomolecules or ions in the cell are not without precedent.[26,27] For example, a recent molecular dynamics study showed that nonspecific protein−protein interactions can lead to the accumulation of non-native or partially unfolded intermediates, suggesting that the unfolded state is enthalpically stabilized by such interactions (the simulations did not address the entropic effect of multiple crowders).[28] If the unfolded state is less compact in mitotic cells, it may make more such stabilizing interactions (lower enthalpy, as observed), while being pinned down more due to such interactions (lower entropy, as observed). As another example, a statistical mechanical model[29] has shown that attractive interactions between protein and crowder can counteract excluded volume effects. And of course, many *in vitro* studies have shown that protein folding enthalpies depend on ionic strength.[1] Finally, previous in cell studies have shown that the stabilization imparted from moving a protein from *in vitro* to the cytoplasm can vary widely from a net stabilizing effect,[15] virtually no effect on stability,[30,31] and destabilization.[32,33] Such protein-specific effects implicate the importance of ionic or hydrophobic interactions between a protein and its surrounding environment, which evidence has shown are sequence dependent in cells.[34] Nonetheless, it is worth pointing out again that the overall effect of in-cell crowding on PGK is stabilizing in both mitotic and interphase cells relative to *in vitro*, and the balance of enthalpic and entropic contributions plays a role in fine-tuning stability as a function of the cell cycle.

(3). Some of the effects we observe here are consistent with both energy landscape and spatial variations of PGK folding in the cell. For example, consider our measurement of β averaged over the whole cell. Kinetics with $\beta < 1$ might simply reflect spatial averaging over a distribution of two-state rate coefficients inside the cell, indicating spatial heterogeneity. In that scenario, mitotic cells with smaller β are more spatially heterogeneous than interphase cells. On the other hand, the variation of β could also be caused by enthalpic stabilization of unfolded states in mitotic cells, as discussed above: Stabilization of folding intermediates would lead to a departure from two-state folding signaled by $\beta < 1$. In that scenario, mitotic cells could be spatially homogeneous, but the energy landscape of the protein has changed toward multistate folding throughout the cell. The two scenarios are not inconsistent with one another, and both spatial and energy landscape variations are likely to exist within the cell.

To see if we could detect spatial variations of folding during the cell cycle, we measured folding kinetics in both DNA-rich and DNA-poor columns within mitotic cells, which have dissolved the nuclear envelope, but show condensed nuclear material (Figure 4). Previous work has shown that PGK-FRET localized to the nucleus of interphase cells is more stable and folds more rapidly than in the cytoplasm.[10] Therefore, it was postulated that nuclear DNA−protein interaction could be responsible for faster folding and greater stability. We found that although there is a very weak trend toward faster folding close to the mitotic chromosomes, this difference cannot account for the faster folding observed in mitotic cells, nor is it as large as that observed between nucleus and cytoplasm of interphase cells. Thus, the loss of nuclear compartmentalization results in greater spatial homogeneity of the folding environment in mitotic cells than in interphase cells. We therefore conclude that the smaller β in mitotic cells is either due to cell cycle variation of the folding energy landscape, consistent with our scenario of less crowding and enthalpic stabilization of unfolded states in mitotic cells, or if it is due to spatial heterogeneity, the latter must be at the level of cellular microstructure below a few micrometers.

■ OUTLOOK

The methodology developed here enables future studies of the time-dependence of the in-cell folding landscapes of other proteins. Of particular interest in the field of molecular biology is the study of cell-cycle related proteins. An intriguing possibility raised by our results is that of protein regulation by functional energy landscape or folding energy landscape modulation: could a protein that is active in interphase be thermodynamically stabilized in that phase of the cell cycle and destabilized in others, or *vice versa*? Our results here are of particular importance to proteins with transient structural elements such as intrinsically disordered proteins. In these cases, modulations of the energy landscape of just ∼5 kJ/mol observed here (based on ΔT_m in Figure 2 and δg_1 in Table 1, $\Delta\Delta G = \Delta T_m\ \delta g_1$) could have dramatic effects on a protein's structure, stability, or function, thanks to the amplifying effect of the exponential Boltzmann factor $\exp[-\Delta\Delta G/RT]$. Considering our results, these types of proteins may be far

dx.doi.org/10.1021/ja4087165 | J. Am. Chem. Soc. 2013, 135, 19215−19221

more structurally dynamic with respect to time in their native cellular environment than expected, especially if the cell places them near structural transitions to begin with.

■ ASSOCIATED CONTENT

Supporting Information

Additional details of the experimental measurements and data analysis. This material is available free of charge via the Internet at http://pubs.acs.org.

■ AUTHOR INFORMATION

Corresponding Author

*E-mail: mgruebel@illinois.edu.

Notes

The authors declare no competing financial interest.

■ ACKNOWLEDGMENTS

Financial support was provided by the National Science Foundation Grant MCB 10-19958. A.J.W. is supported by the NSF Graduate Research Fellowship under grant number DGE-1144245. The authors thank Hannah Gelman and Minghao Guo for instrument support and technical assistance.

■ ABBREVIATIONS

PGK-FRET, FRET-labeled yeast phosphoglycerate kinase; FRET, Forster resonance energy transfer

■ REFERENCES

(1) Record, M. T., Jr.; Zhang, W.; Anderson, C. F. In *Advances in Protein Chemistry*; Richards, F. M., Eisenberg, D. S., Kim, P. S., Eds.; Academic Press: Waltham, 1998; Vol. *51*, p 281.
(2) Zhou, H.-X.; Rivas, G.; Minton, A. P. *Annu. Rev. Biophys.* **2008**, *37*, 375.
(3) Rosgen, J.; Pettitt, B. M.; Bolen, D. W. *Biophys. J.* **2005**, *89*, 2988.
(4) Gelman, H.; Platkov, M.; Gruebele, M. *Chem.—Eur. J.* **2012**, *18*, 6420.
(5) Pardee, A. B.; Dubrow, R.; Hamlin, J. L.; Kletzien, R. F. *Annu. Rev. Biochem.* **1978**, *47*, 715.
(6) Kubbutat, M.; Jones, S. N.; Vousden, K. H. *Nature* **1997**, *387*, 299.
(7) Watson, H. C.; Walker, N. P. C.; Shaw, P. J.; Bryant, T. N.; Wendell, P. L.; Fothergill, L. A.; Perkins, R. E.; Conroy, S. C.; Dobson, M. J.; Tuite, M. F.; Kingsman, A. J.; Kingsman, S. M. *EMBO J.* **1982**, *1*, 1635.
(8) Dhar, A.; Samiotakis, A.; Ebbinghaus, S.; Nienhaus, L.; Homouz, D.; Gruebele, M.; Cheung, M. S. *Proc. Natl. Acad. Sci. U.S.A.* **2010**, *107*, 17586.
(9) Dhar, A.; Ebbinghaus, S.; Shen, Z.; Mishra, T.; Gruebele, M. *Biophys. J.* **2010**, *99*, L69.
(10) Dhar, A.; Girdhar, K.; Singh, D.; Gelman, H.; Ebbinghaus, S.; Gruebele, M. *Biophys. J.* **2011**, *101*, 421.
(11) Jackman, J.; Connor, P. M. *Curr. Prot. Cell Biol.* **1998**, *8*, 1.
(12) Fitzkee, N.; Rose, G. *Proc. Natl. Acad. Sci. U.S.A.* **2004**, *101*, 12497.
(13) Guo, M. H.; Xu, Y. F.; Gruebele, M. *Proc. Natl. Acad. Sci. U.S.A.* **2012**, *109*, 17863.
(14) Osvath, S.; Herenyi, L.; Zavodszky, P.; Fidy, J.; Kohler, G. *J. Biol. Chem.* **2006**, *281*, 24375.
(15) Osvath, S.; Sabelko, J. J.; Gruebele, M. *J. Mol. Biol.* **2003**, *333*, 187.
(16) Ebbinghaus, S.; Dhar, A.; McDonald, D.; Gruebele, M. *Nat. Methods* **2010**, *7*, 319.
(17) Sabelko, J.; Ervin, J.; Gruebele, M. *Proc. Natl. Acad. Sci. U.S.A.* **1999**, *96*, 6031.
(18) Best, R. B.; Hummer, G. *Proc. Natl. Acad. Sci. U.S.A.* **2010**, *107*, 1088.
(19) Hagen, S. J. *Curr. Protein Pept. Sci.* **2010**, *11*, 385.
(20) Matouschek, A.; Kellis, J. T.; Serrano, L.; Fersht, A. R. *Nature* **1989**, *340*, 122.
(21) Naganathan, A. N.; Munoz, V. *Proc. Natl. Acad. Sci. U.S.A.* **2010**, *107*, 8611.
(22) Weikl, T. R. *Proteins: Struct. Funct. Bioinformatics* **2005**, *60*, 701.
(23) Gierasch, L. M.; Gershenson, A. *Nat. Chem. Biol.* **2009**, *5*, 774.
(24) Cheung, M. S.; Klimov, D.; Thirumalai, D. *Proc. Natl. Acad. Sci. U.S.A.* **2005**, *102*, 4753.
(25) Muramatsu, N.; Minton, A. P. *Proc. Natl. Acad. Sci. U.S.A.* **1988**, *85*, 2984.
(26) Douglas, J.; Dudowicz, J.; Freed, K. *Phys. Rev. Lett.* **2009**, *103*, 135701.
(27) Jiao, M.; Li, H.-T.; Chen, J.; Minton, A. P.; Liang, Y. *Biophys. J.* **2010**, *99*, 914.
(28) Harada, R.; Tochio, N.; Kigawa, T.; Sugita, Y.; Feig, M. *J. Am. Chem. Soc.* **2013**, *135*, 3696.
(29) Kim, Y. C.; Mittal, J. *Phys. Rev. Lett.* **2013**, *110*, 208102(1).
(30) Ignatova, Z.; Gierasch, L. M. *Proc. Natl. Acad. Sci. U.S.A.* **2004**, *101*, 523.
(31) Ignatova, Z.; Krishnan, B.; Bombardier, J. P.; Marcelino, A. M. C.; Hong, J.; Gierasch, L. M. *Biopolymers* **2007**, *88*, 157.
(32) Phillip, Y.; Kiss, V.; Schreiber, G. *Proc. Natl. Acad. Sci. U.S.A.* **2012**, *109*, 1461.
(33) Guzman, I.; Gelman, H.; Tai, J.; Cheung, M. S.; Gruebele, M. *J. Mol. Biol.* **2013**, in press.
(34) Wang, Q.; Zhuravleva, A.; Gierasch, L. M. *Biochemistry* **2011**, *50*, 9225.